Determination of Optimum Welding Parameters for FSW AA2024-T351

Samir Ali Amin Al-Rubaie*   Qasim Abbas Atiah**
Zuhair Altaher***

*, **, *** Department of Mechanical Engineering / University of Technology
*E-mail: alrabiee2002@yahoo.com
**E-mail: dr_qasim_uot@yahoo.com
***E-mail: zuhairsadeed@gmail.com

Abstract

Friction stir welding is a relatively new joining process, which involves the joining of metals without fusion or filler materials. In this study, the effect of welding parameters on the mechanical properties of aluminum alloys AA2024-T351 joints produced by FSW was investigated.

Different ranges of welding parameters, as input factors, such as welding speed (6 - 34 mm/min) and rotational speed (725 - 1235 rpm) were used to obtain their influences on the main responses, in terms of elongation, tensile strength, and maximum bending force. Experimental measurements of main responses were taken and analyzed using DESIGN EXPERT 8 experimental design software which was used to develop the response surface methodology (RSM) models. Mathematical model of responses, as functions of used welding conditions, were obtained and analyzed by ANOVA variance to verify the adequacy of these models. The resultant quadratic models showed that as the rotation speed or welding speed increases, the tensile strength and elongation of the joint firstly increase to a maximum value and then decrease more likely due to the occurrence of void defect. Increasing both welding speed and rotational speed leads to increase the maximum bending force firstly to a maximum value and then decreases. However, the welding speed was found more significant than rotational speed. A good agreement was found between the results of these models and optimization with the experimental ones with confidence level of 95%.

Keywords: Friction stir welding, DOE, RSM, Mechanical properties, Modeling and Optimization .

1. Introduction

Friction stir welding (FSW) is a solid-state joining technology invented at the welding institute (TWI) in 1991. It has been proven to be a very successful joining technology for aluminum alloys. Compared to the conventional welding processes, FSW can produce superior mechanical properties in the weld zone. This new technique is attracting more and more research interest [1].

The FSW process appears to offer a number of advantages over conventional fusion welding techniques, such as no need for expensive consumables such as filler wire and gas shields, ease of automation on simple milling machinery, good mechanical properties of the resultant joint, and low distortion [1].

During the FSW process, the tool penetrates into the workpiece, and then moves along the joint line at a constant speed (see Figure 1). The material in front of the rotating tool pin is plastically deformed and stirred back to the trail edge of the tool pin in the welding.

The tool serves three primary functions, that is, heating of the workpiece, movement of material to produce the joint, and containment of the hot metal beneath the tool shoulder. Heating is created within the workpiece both by friction between the rotating tool pin and shoulder and by severe plastic deformation of the workpiece. The localized heating softens the material around the

pin and, combined with the tool rotation and translation, leads to movement of material from the front to the back of the pin, thus filling the hole in the tool wake as the tool moves forward. The tool shoulder restricts the metal flow to a level equivalent to the shoulder position, that is, approximately to the initial workpiece top surface.

As a result of the tool action and influence on the workpiece, when performed properly, a solid state joint is produced, that is no melting. Because of various geometrical features on the tool, material movement around the pin can be complex, with gradients in strain, temperature, and strain rate. Accordingly, the resulting nugget zone microstructure reflects these different thermomechanical histories and is not homogeneous [1].

A lot of researches [2-7] has been already done towards understanding the effect of FSW process parameters on the material flow behavior, microstructure formation, tool design and mechanical properties of friction stir welded joints, but there is a few works on studying the influence of input factors on mechanical properties using design of experiments (DOE) and response surface methodology (RSM) technique.

In this investigation, an attempt has been made to determine the effect of FSW process parameters on mechanical properties (elongation, tensile strength, and maximum bending force) in Al alloy (AA2024-T351).

2. Experimental Work

2.1. Selecting the aluminum alloy and specimens preparation of plates

The base material used in this investigation is 2024-T351 which was obtained from a local market with thickness of (3.2 mm). AA2024-T351 aluminum alloy is Al-Cu-Mg grade alloy of 2xxx series heat treatable of medium strength alloys. A piece of this alloy was analyzed to find its chemical composition by spectro device, as shown in Table 1 with the standard material according as ASTM B209M [8] and the standard mechanical properties of AA2024-T351 aluminum alloy, given in Table 2.

The base material cut into required size is (210 mm *110 mm *3.2 mm) by a power saw cutting convenient for conducting FSW, and the plate edge was ground to ensure that there is no gap between the two plates.

2.2. Design and Manufacturing of Welding Tools

The design of the tool is the key to the successful application of the process to a greater range of material and over a wider range of thickness.

FSW tool of square pin profile and straight cylindrical shoulder was used. The geometry and dimensions of the tool are pin rotational diameter of 5 mm, shoulder diameter of 15 mm and pin length of 2.7 mm, see Figure 2. The friction stir welding tool was manufactured by CNC turning and milling machines, this friction stir welding tool was fabricated from tool steel labeled as X12M (density ρ = 7800 kg/m^3, specific heat C_p = 500 J/kg.^{o}C and the thermal conductivity k = 40 W/m.^{o}C). The tool heat treatment includes heating the metal to 1020°C for 30 min and then air cooling to room temperature, which gives a hardness of 58 HRC [9], its chemical composition is tabulated in Table 3 together with the standard tool material.

2.3. Selecting the Optimum FSW Process Parameters

To obtain high quality of friction stir welded joints with high mechanical properties, i.e., high welding efficiency, the main welding parameters (rotational speed and welding speed) must be selected to determine the effect of each parameter on the mechanical properties.

The rotational and welding speeds were chosen, therefore the tool rotational speed (725 - 1235 rpm) and the welding speed (6-34 mm/min) were used (see Table 4). The FSW tests were carried out on a vertical milling machine with a square butt joint configuration.

All the welds were produced perpendicularly to the rolling direction for aluminum alloys.

2.4. Welding Procedure

A plate was fixed at a predetermined location on the backing plate (which was a 280*280*25 mm steel plate) and clamped into place. This same location was used for all plates in this study. The tool was then positioned directly over the plunge location and the pin was brought into contact with the top surface of the workpiece, see Figure 3.

Each tool plunges slowly between the two sheets that are required to be welded until the

shoulder of the tool touches the sheet surface. The tool was then allowed to dwell for 30-40 sec to allow the shoulder to preheat the workpiece during welding. After the dwell, the tool began to traverse along the welding line with the selected tool. When a full weld has been made, the pilot hole will be welded over and the pin was parked above the weld. When the tool was parked, it was dragged, and a park hole was left, as shown in Figure 4.

2.5. Mechanical Tests

2.5.1. Tensile Test

Tensile test was carried out on samples taken in a perpendicular direction to the welding to determine the tensile properties of the welding joints, see Figure 5. The shape and dimensions of the transverse tensile specimens according to ASTM E 8M [10] are shown in Figure 6. All tensile tests were carried out at room temperature and constant loading rate (5 mm/min) by a computerized universal testing machine (Hydraulic Tinius Olsen), which has a maximum capacity of (1000 kN). Then, the average of three specimens was taken to evaluate the tensile behavior of each welded joint.

2.5.2. Bending Test

Three point bending test was carried out to determine the maximum bending force of the welded joints. Bending tests were conducted with former diameter equal to 30 mm. The shape and dimensions of the transverse bending specimens are (15.24 mm * 38.1 mm) according to ASTM E 190 [11]. The bending test was carried out at room temperature by a universal testing machine (Hydraulic LARYEE testing machine).

3.   Response Surface Methodology (RSM)

Response surface methodology (RSM) is a collection of mathematical and statistical techniques that are used for empirical model building and analysis of problems, in which a response of interest is influenced by several variables, and the objective is to optimize this response [12]. It has been extensively used in different engineering applications and fields. RSM is important in designing, formulating, developing, and analyzing new scientific studying

and products. It is also efficient in the improvement of existing studies and products. The application of RSM to design optimization is aimed at reducing the cost of expensive analysis methods (e.g., finite element method or CFD analysis) and their associated numerical noise. By careful design of experiments, the objective is to optimize a response (output variable) which is influenced by several independent variables (input variables). An experiment is a series of tests, called runs, in which changes are made in the input variables in order to identify the reasons for changes in the output response. The advantages of design of experiments, as reviewed by Aggarwal and Singh [13], are as follows: (1) Numbers of trials are reduced. (2) Optimum values of parameters can be determined. (3) Assessment of experimental error can be made. (4) Qualitative estimation of parameters can be made. (5) Inference regarding the effect of parameters on the characteristics of the process can be made.

The efficiency of RSM is significantly influenced by selecting the proper choice of experimental designs. The central composite design (CCD) is one of the most popular class of designs to fit response surfaces, building the second order (quadratic) regression model to predict the responses. Also, the most important characteristics of CCD is the spherical or rotatability property, i.e., the variance of predicted responses is the same at all points that are the same distance from the design center.

Therefore, in the present research, RSM was utilized using CCD to establish predicted models for some responses (mechanical properties) as functions of input factors (welding speed and rotational speed) during FSW process of 2024-T351 Aluminum alloy using the optimum tool design.

Moreover, numerical optimization was used to optimize the input parameters to obtain maximum responses.

4.   Experimental Design Matrix

The input parameters used in the whole experimentation were selected according to the practical experience and the limitations of the experimental measurements. These factors are given in Table 4 with two levels. The experimental design used was the response surface methodology using a central composite rotatable design for 2^2 factors, with 5 central points and $\alpha = \pm1.414$. 13 runs were performed according to the experimental design matrix (5

center points). Each parameter was used at different code levels of −1.414, −1, 0, +1, and +1.414, whereby each level used conformed to an actual value equivalent to the coded value.

Thus, the input parameters studied are welding speed and rotational speed. The experimental design matrix used for input parameters in terms of actual factors with the experimental values of elongation, tensile strength and maximum bending load is given in Table 5. The software DESIGN EXPERT 8 was used to develop the model. Results of test runs are reported, as well as, the prediction models produced within a 95% confidence interval.

5. Results and Discussion

5.1. Tensile and Bending Test Results

After carrying out the experiments, the welded joints were visually examined and the welds with good surface appearance were chosen and machined into the standard test specimens for the mechanical testing (according to ASTM E8M [10] for tensile test and ASTM E190 [11] for bending test).

Tensile and bending tests were carried out as shown in Figures 7a, 7b, and 8. It should be noted that the testing values of tensile and bending for the base metal are (438 MPa) and (1520 N), respectively.

5.2. Modeling of the Elongation

The average responses obtained for elongation, tensile strength and maximum bending load were used in calculating the models of the response surface per response using the least-squares method.

For elongation prediction, a reduced quadratic model in coded terms was analyzed with backwards elimination of insignificant coefficients at an exit threshold of alpha = 0.1. Some coefficients were removed in order to obtain a formula with actual factors rather than coded ones. The term removed was AB. This means that the interaction of welding speed and rotational speed term had no significant effect on the elongation.

Table 6 shows the statistical analysis of variance produced by the software for the remaining terms. The model is significant at 95% confidence. It is noted that the rotational speed

(B), squared welding speed (A^2), and the squared rotational speed (B^2) terms are all significant, while the welding speed (A) term is not. The lack of fit test indicates a good model. This model illustrates that only the three terms (B, A^2 and B^2) have the highest impact on elongation. The final equation in terms of coded factors is :

$$\text{Elongation} = +4.12 - 0.016 * A + 0.61 * B - 0.70 * A^2 - 1.25 * B^2 \qquad \ldots(1)$$

And, the final equation in terms of actual factors is:

$$\text{Elongation} = -39.12769 + 0.28011 * \text{Welding speed} + 0.079162 * \text{Rotational speed} - 7.04170E\text{-}003 * \text{Welding speed}^2 - 3.86475E\text{-}005 * \text{Rotational speed}^2 \qquad \ldots(2)$$

Looking at the normal probability plot (Figure 9a) for the elongation data, the residuals generally that falling on a straight line implying errors, are normally distributed. Also, according to Figure 9b that depicts the residuals versus predicted responses for elongation data, it is seen that no obvious patterns or unusual structure, implying models are accurate.

Figure 9c exhibits that the contour graph of welding speed and elongation as a response. It is seen that the increase in both welding speed and rotational speed leads to increase the elongation. The increase in welding speed led to increase in elongation. The joint exhibits poor elongation at a lower welding speed of 10 mm/min owing to the larger heat generation. As the welding speed increases from 10 to 20 mm/min, the negative effects of thermal cycles on joint properties are weakened, leading to an improvement in elongation. Between 20 and 30 mm/min, the elongation of the joints show a decrease with increasing welding speed due to the occurrence of void defect. Also, the increase in rotational speed led to increase in elongation. It can be seen that the elongation of the joint increases with increasing the rotational speed from 800 rpm to 980 rpm. The reason for this can be explained as follows: increasing the rotational speed would extend the shoulder dominated zone over the plate thickness. Since the material in this shoulder dominated zone is softer and easier to be stirred, extending this zone through the thickness enhances the stirring and consequently improves the elongation of the joints. However, when the rotational speed increases up to 1160 rpm, the elongation of the joint decreases because of the formation of void defect.

Figure 10 manifests the predicted actual elongation data versus the actual ones for

comparison reason. While Figure 11 shows the 3D graph of elongation as a function of welding speed and rotational speed. It can be noted that the increase of welding speed resulted in a slight increase in the elongation value, while the increase of rotational speed caused a higher increase in the elongation. This means that the rotational speed has the highest impact on the elongation value. In other words, the rotational speed is more significant than the welding speed in the elongation model.

With increasing rotational speed for a fixed welding speed or increasing welding speed for a fixed rotational speed, the elongation of the joints firstly increased to a maximum value and then showed a decrease due to the occurrence of welding defects [6, 14].

5.3. Modeling of the Tensile Strength

Similarly, for tensile strength measurements, a reduced quadratic model in coded terms was analyzed with backwards elimination of insignificant coefficients at the exit threshold of alpha = 0.1. The term removed was AB for obtaining a formula with actual factors rather than coded ones.

Table 7 reveals the statistical analysis of variance (ANOVA), and this model is significant at 95% confidence. The rotational speed (B), squared welding speed (A²) and the squared rotational speed (B²) terms are all significant, while the welding speed (A) term is not. This model indicates that these three terms have the highest impact on the tensile strength. The lack of fit test indicates a good model. The final equation in terms of coded factors is :

Tensile strength = +230.40 + 3.14 * A -16.91 * B - 22.40 * A^2 -27.35 * B^2 …(3)

The final equation in terms of actual factors is:

Tensile strength = -584.03137 + 9.27514 * Welding speed + 1.56032 * Rotational speed - 0.22402 * Welding $speed^2$ - 8.44003E-004 * Rotational $speed^2$ …(4)

The normal probability plot of residuals for tensile strength data shows that the residuals (errors) fall generally on a straight, and they are normally distributed. And, there are no obvious patterns or unusual structure, implying models are accurate.

According to Figure 12 for the contour graph, it can be noticed that the increase of both welding

speed and rotational speed generally increase the tensile strength value. Figure 13 depicts the predicted versus actual tensile strength data for comparison purpose. Whereas, Figure 14 reveals the 3D graph of tensile strength as a function of welding speed and rotational speed. It is seen that the increase in both welding speed and rotational speed leads to increase the tensile strength. The increase in welding speed led to increase in tensile strength. The joint exhibits poor tensile strength at a lower welding speed of 10 mm/min owing to the larger heat generation. As the welding speed increases from 10 to 20 mm/min, the negative effects of thermal cycles on joint properties are weakened, leading to an improvement in tensile strength. Between 20 and 30 mm/min, the tensile strength of the joints shows a decrease with increasing welding speed due to the occurrence of void defect. Also, the increase in rotational speed led to increase in tensile strength. It can be seen that the tensile strength of the joint increases with increasing the rotational speed from 800 rpm to 980 rpm. The reason for this can be explained as follows: increasing the rotational speed would extend the shoulder dominated zone over the plate thickness. Since the material in this shoulder dominated zone is softer and easier to be stirred, extending this zone through the thickness enhances the stirring and consequently improves the tensile strength of the joints. However, when the rotational speed increases up to 1160 rpm, the elongation of the joint decreases because of the formation of void defect.

With increasing rotational speed for a fixed welding speed or increasing welding speed for a fixed rotational speed, the elongation of the joints firstly increased to a maximum value and then showed a decrease due to the occurrence of welding defects [6, 14].

5.4. Modeling of the Maximum Bending Force

Similarly, for maximum bending force measurements, a reduced quadratic model in coded terms was analyzed with backwards elimination of insignificant coefficients at the exit threshold of alpha = 0.1. The term removed was AB for obtaining a formula with actual factors rather than coded ones.

Table 8 reveals the statistical analysis of variance (ANOVA), and this model is significant at 95% confidence. The welding speed(A), squared welding speed (A²) and the squared

rotational speed (B²) terms are all significant, while the rotational speed (B) is not significant. This model illustrates that these three terms have the highest impact on the tensile strength. The lack of fit test indicates a good model. The final equation in terms of coded factors is :

Maximum bending force = + 1374.98 + 61.68 * A - 20.39 * B - 320.89 * A^2 -322.80 * B^2 …(5)

The final equation in terms of actual factors is:

Maximum bending force = -9489.29985 + 134.52393 * Welding speed + 19.41404 * Rotational speed - 3.20890 * Welding speed^2 - 9.96292E-003 * Rotational speed^2 …(5.6)

The normal probability plot of residuals for maximum bending force data shows that the residuals (errors) fall generally on a straight, and they are normally distributed. And, there are no obvious patterns or unusual structure, implying models are accurate.

According to Figure 15 for the contour graph showing the interaction of welding speed and rotational speed, it can be noticed that the increase of both welding speed and rotational speed generally increase the maximum bending force value. Figure 16 depicts the predicted versus actual maximum bending force data for comparison purpose. Whereas, Figure 17 reveals the 3D graph of maximum bending force as a function of welding speed and rotational speed. It is seen that the increase in welding speed leads to increase the maximum bending force. As indicated with the elongation and tensile strength models, it can be concluded that the maximum bending force is also smaller at the lowest and highest welding speed and rotational speed, whereas it is larger at (20 mm/min) welding speed and (980 rpm) rotational speed.

5.5. Numerical Optimization of Elongation, Tensile Strength and Maximum Bending Force

The numerical optimization was provided by the Design of Experiment software to find out the optimum combinations of parameters in order to fulfill the requirements as desired. Therefore, this software was used for this optimization, based on the data from the predictive models for three responses, elongation, tensile strength and maximum bending force, as a function of two factors: welding speed and rotational speed. Elongation, tensile strength and maximum

bending force are modeled with a quadratic model.

To develop the new predicted models, a new objective function, named Desirability which allows to properly combining all the goals, was evaluated. Desirability is an objective function, to be maximized through a numerical optimization, which ranges from zero to one at the goal. Adjusting its weight or importance may alter the characteristics of a goal, and the aim of the optimization is to find a good set of conditions that will meet all the goals. Usually, the weights are used to establish an evaluation of the goal's 3D importance when maximizing desirability function; in this work, weights are not changed since the three responses (elongation, tensile strength and maximum bending force) have the same importance and are not in conflict within each other.

The ultimate goal of this optimization was to obtain the maximum response that simultaneously satisfied all the variable properties. Table 9 lists the constrains of each variable for numerical optimization of the elongation, tensile strength and maximum bending force. According to this table, one possible run fulfilled these specified constrains to obtain the optimum values for elongation, tensile strength and maximum bending force, as given in Table 10. It can be seen that this run gave desirability of 0.868. Figure 18 shows the surface plot for desiability as a function of welding speed and rotational speed. Figures 19,20 and 21 depict the optimum values of the elongation, tensile strength and maximum bending force, respectively. Thus, it can be concluded from these figures that the desirability reaches the maximum value of 0.868 when the optimum value of elongation is 4.1 % (Figure 19), the optimum value of tensile strength is 230.773 MPa (Figure 20) and the optimum value of maximum bending force is 1377.83 N, as shown in (Figure 21).

5.6. Comparison of Predicted Results with Experimental Ones

A comparison between the actual (with the optimum tool design) and predicted for elongation, tensile strength, and maximum bending force is shown in Table 11. This table also exhibits the percentage error between the actual and predicted results of elongation, tensile strength, and maximum bending force. In addition, according to this table, it is shown a very

good agreement between the actual results of the elongation, tensile strength, and maximum bending force and the predicted results obtained by DOE and RSM technique.

6. Conclusions

The following conclusions have been made from the present investigation:
- Increasing both welding speed and rotational speed leads to increase the elongation and tensile strength up to 20 mm/min welding speed and 980 rpm rotational speed. The increase of welding speed resulted in a slight increase in the elongation and tensile strength, while the increase of rotational speed caused a higher increase in these two properties. This means that the rotational speed has the highest impact than welding speed on the elongation and tensile strength.
- Increasing both welding speed and rotational speed leads to increase the maximum bending force up to 20 mm/min welding speed and 980 rpm rotational speed. However, the welding speed was found more significant than rotational speed.
- Quadratic predicted models for elongation, tensile strength, and maximum bending force were obtained in terms of welding speed and rotational speed with 95% confidence level.
- Among the 13 experiments of experimental work, 20 mm/min welding speed and 980 rpm rotational speed gives better tensile strength (245 MPa), elongation (4.7), maximum bending force (1450 N).
- From the numerical optimization, the optimum values of elongation, tensile strength, and maximum bending force were found to be (4.1%), (230.733MPa) and (1377.83 N), respectively with a desirability 0.868 at (21 mm/min) welding speed and (977 rpm) rotational speed.

Table 1,
Standard and experimental chemical compositions of aluminum alloy AA2024-T351 (wt%).

Material	wt%						
	Si	Fe	Cu	Mn	Mg	Cr	Zn
Standard [8]	≤0.500	≤0.500	3.800-4.900	0.300-0.900	1.200-1.800	≤0.100	≤0.250
Experimental	0.121	0.265	3.800	0.511	1.370	0.009	0.134

Table 2,
Standard and experimental mechanical properties of aluminum alloy AA2024-T351.

Material	Property		
	$б_y$ (Mpa)	$б_u$ (Mpa)	EL. (%)
Standard [8]	≥290	≥435	≥15
Experimental	327	438	17.3

Table 3,
Chemical composition of tool steel X12M [8].

Element	C	Si	Mn	P	S	Cr	Cu	Ni	V
Standard [9]	1.800 - 2.400	≤0.400	≤0.600	≤0.030	≤0.030	12.000 - 15.000	≤0.250	≤0.500	≤0.300
Actual	1.870	0.278	0.270	0.009	0.001	12.440	0.079	0.200	0.023

Table 4,
Levels of Input Parameters Used with Respective Coding.

Factor	Unit	Low Level (-1)	High Level (+1)	-alpha (-1.414)	+alpha (+1.414)
Welding Speed	mm/min	10	30	6	34
Rotational Speed	rpm	800	1160	725	1235

Table 5
Experimental design matrix for both actual input factors and responses.

Standard No.	Run No.	Type of Point	Welding Speed (mm/min)	Rotational Speed (rpm)	Elongation (%)	Tensile Strength (MPa)	Maximum Bending force (N)
1	3	Factorial	10	800	1.1	206	673
2	13	Factorial	30	800	1.5	206	838
3	6	Factorial	10	1160	2.6	161	670
4	9	Factorial	30	1160	2.5	172	787
5	1	Axial	6	980	3.1	175	775
6	10	Axial	34	980	2.8	185	790
7	2	Axial	20	725	1.0	190	550
8	4	Axial	20	1235	2.7	150	715
9	7	Center	20	980	3.5	218	1330
10	8	Center	20	980	4.7	245	1450
11	5	Center	20	980	4.2	217	1350
12	11	Center	20	980	3.7	231	1316
13	12	Center	20	980	4.5	241	1435

Table 6
ANOVA Analysis for Response Surface Quadratic Model (Elongation, %).

Source	Sum of squares	df	Mean square	F value	p-value Prob > F
Model	16.01	4	4.00	19.62	0.0003 significant
A- Welding speed	1.930E-003	1	1.930E-003	9.464E-003	0.9249
B- Rotational speed	3.02	1	3.02	14.82	0.0049
A^2	3.45	1	3.45	16.91	0.0034
B^2	10.94	1	10.94	53.62	< 0.0001
Residual	1.63	8	0.20		
Lack of Fit	0.58	4	0.15	0.56	0.7077 not significant
Pure Error	1.05	4	0.26		
Cor Total	17.64	12	17.64		

Std. Dev.	0.45	R-Squared	0.9075
Mean	2.92	Adj R-Squared	0.8612
C.V.%	15.49	Pred R-Squared	0.7552
Press	4.32	Adeq Precision	12.044

Table 7
ANOVA Analysis for Response Surface Quadratic Model (Tensile strength, MPa).

Source	Sum of squares	df	Mean square	F value	p-value Prob > F
Model	10100.35	4	2525.09	20.08	0.0003 significant
A- Welding speed	79.02	1	79.02	0.63	0.4508
B- Rotational speed	2288.39	1	2288.39	18.20	0.0027
A^2	3490.78	1	3490.78	27.76	0.0008
B^2	5215.56	1	5215.56	41.48	< 0.0002
Residual	1005.96	8	125.74		
Lack of Fit	346.76	4	86.69	0.53	0.7255 not significant
Pure Error	659.20	4	164.80		
Cor Total	11106.31	12			

Std. Dev.	11.21	R-Squared	0.9094
Mean	199.77	Adj R-Squared	0.8641
C.V.%	5.61	Pred R-Squared	0.7626
Press	2636.86	Adeq Precision	11.335

Table 8
ANOVA Analysis for Response Surface Quadratic Model (Maximum bending force, N).

Source	Sum of squares	df	Mean square	F value	p-value Prob > F
Model	1.310E+006	4	3.275E+005	110.86	< 0.0001 significant
A- Welding speed	30433.08	1	30433.08	10.30	0.0124
B- Rotational speed	3329.39	1	3329.39	1.13	0.3194
A^2	7.162E+005	1	7.162E+005	242.47	< 0.0001
B^2	7.268E+005	1	7.268E+005	246.03	< 0.0001
Residual	23631.56	8	2953.95		
Lack of Fit	6931.56	4	1732.89	0.42	0.7924 not significant
Pure Error	16700.00	4	4175.00		
Cor Total	1.334E+006	12			

Std. Dev.	54.35	R-Squared	0.9823
Mean	978.69	Adj R-Squared	0.9734
C.V.%	5.55	Pred R-Squared	0.9555
Press	59333.04	Adeq Precision	21.628

Table 9
Constrains of each varaible for numerical optimization of Elongation, Tensile strength and Maximum bending force.

Types of variables	Goal	Lower Limit	Upper Limit	Lower Weight	Upper Weight	Importance
A: Welding speed	Is in range	10	30	1	1	3
B: Rotational speed	Is in range	800	1160	1	1	3
Elongation	maximize	1	4.7	1	1	3
Tensile Strength	maximize	150	245	1	1	3
Maximum bending force	maximize	600	1450	1	1	3

Table 10
Optimal conditions used to obtain the maximum Elongation, Tensile strength and Maximum bending force.

No.	Welding Speed (mm/min)	Rotational Speed (rpm)	Elongation (%)	Tensile Strength (MPa)	Maximum Bending force (N)	Desirability
1	21	977	4.1	230.733	1377.83	0.868 selected

Table 11
Comparison between the actual and predicted responses.

	Welding Speed (mm/min)	Rotational Speed (rpm)	Elongation (%)	Tensile Strength (MPa)	Maximum Bending force (N)
Actual	20	980	4.7	245	1450
Predicted	21	977	4.1	230.733	1377.83
% Error	-	-	12.77	5.82	4.98

Table 12
Conversions for each of the units used in the present work.

Unit with SI	Unit with U.S. customary (nonmetric)
1 MPa	145.038 psi
1 m	3.2808 ft
1 mm/min	0.05468 ft/s
1 N	0.2248 Ibf
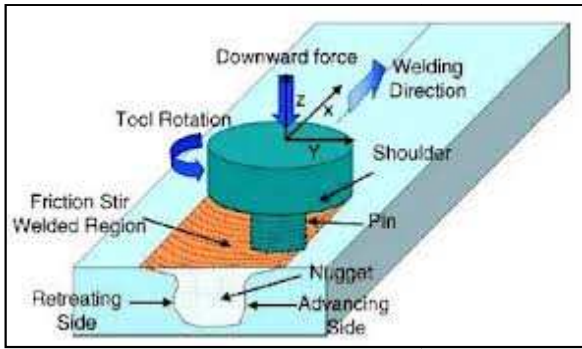
Fig. 1. Schematic diagram of FSW.
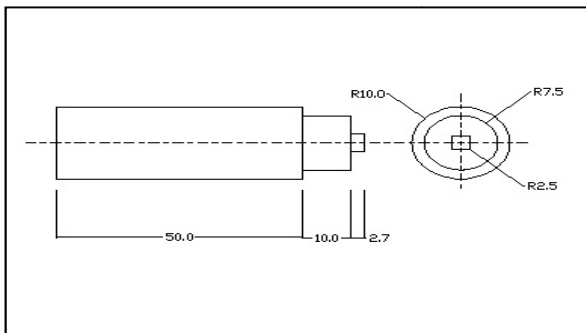
Fig. 2. Design drawing for FSW tool (square pin with flat surface shoulder).

Fig. 3. Welding backing plate and fixtures in use for FSW.
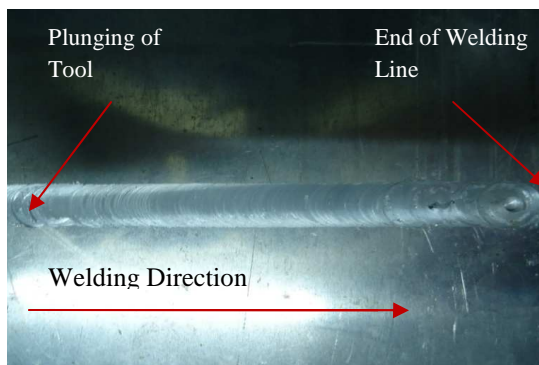
Fig. 4. Welded sample explained welding direction, start, and end of welded joint.
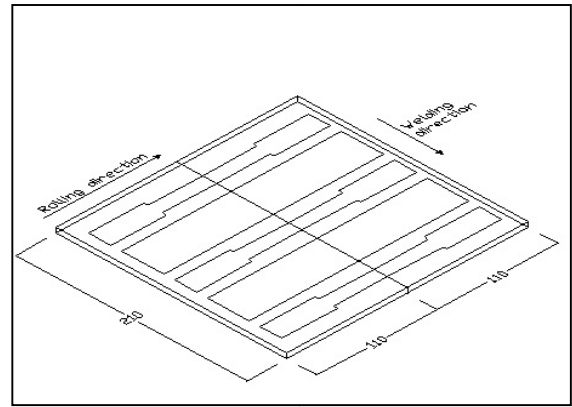
Fig. 5. Tensile and bending test specimens locations (all dimensions in mm).
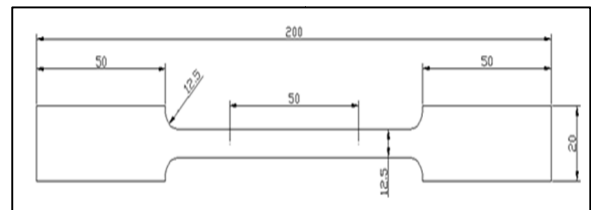
Fig. 6. Tensile test specimen (all dimensions in mm) ASTM (E 8M).

Fig. 7a. Tensile test specimens before testing.

Fig. 7b. Tensile test specimens after testing.

Fig. 8. Bending test specimen after testing.
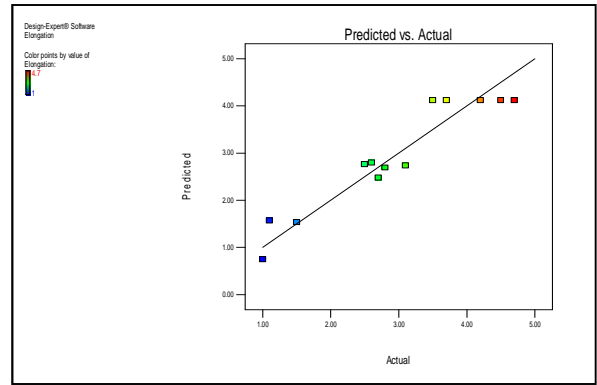
Fig. 10. Predicted versus actual Elongation (%) data for comparison.

Fig. 11. 3D graph of Elongation (%) as a function of welding speed and rotational speed.

Fig. 12. Contour graph of Tensile strength as a function of welding speed and rotational speed.
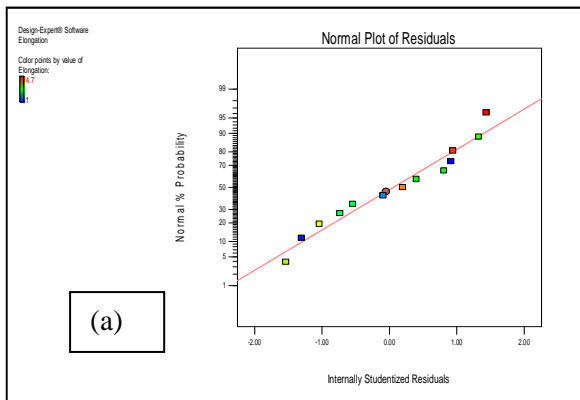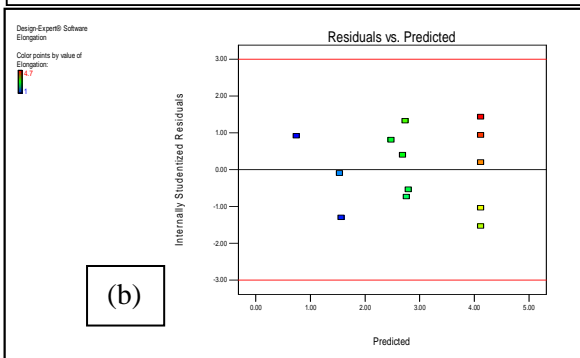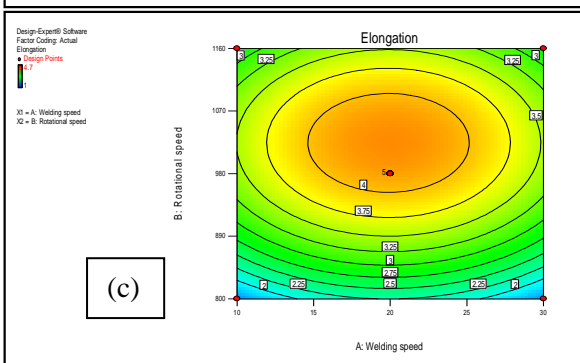
Fig. 9. Modeling of elongation property: (a) Normal probability plot for Elongation (%) data, (b) Residual versus predicted responses Elongation (%) data, and (c) Contour graph of Elongation (%) as a function of welding speed and rotational speed.
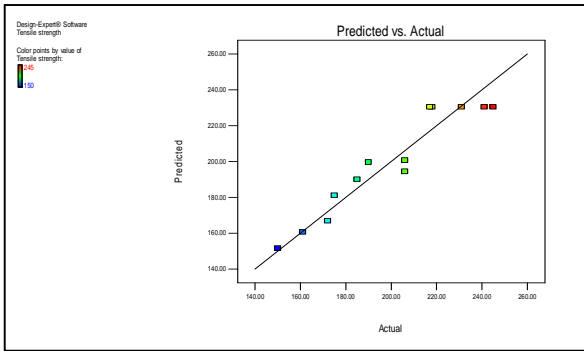
Fig. 13. Predicted versus actual Tensile strength data for comparison.
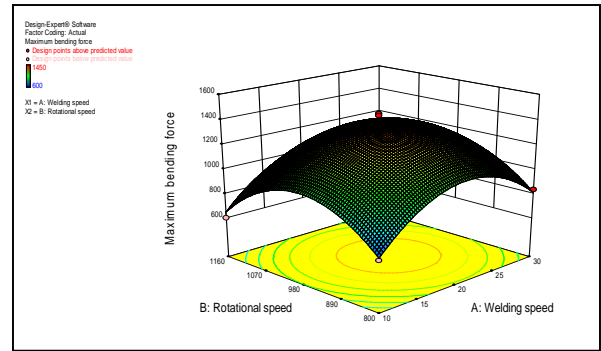
Fig. 17. 3D graph of maximum bending force as a function of welding speed and rotational speed.
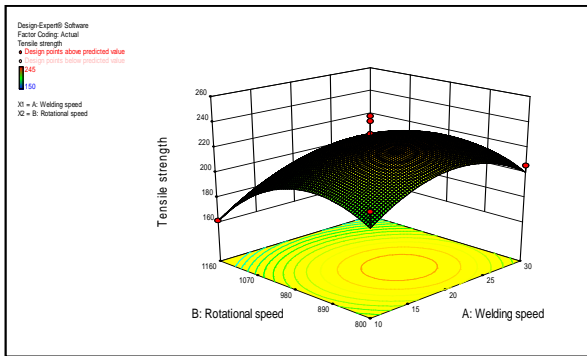
Fig. 14. 3D graph of Tensile strength as a function of welding speed and rotational speed.
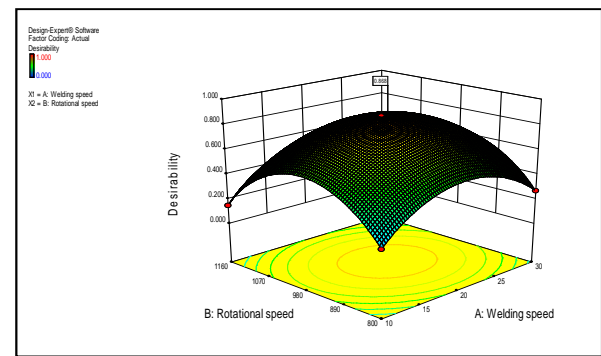
Fig. 18. 3D surface plot for desirability as a function of welding speed and rotational speed.
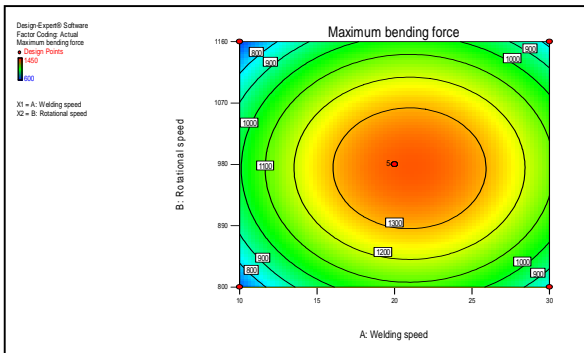
Fig. 15. Contour graph of maximum bending force as a function of welding speed and rotational speed.
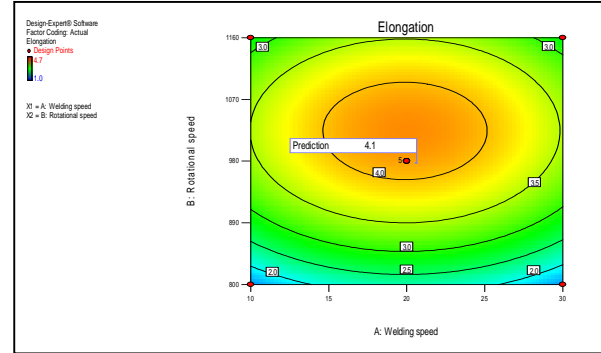
Fig. 19. The optimum value of Elongation.
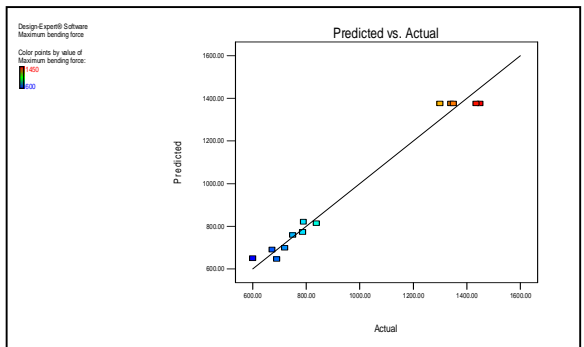
Fig. 16. Predicted versus actual maximum bending force data for comparison.
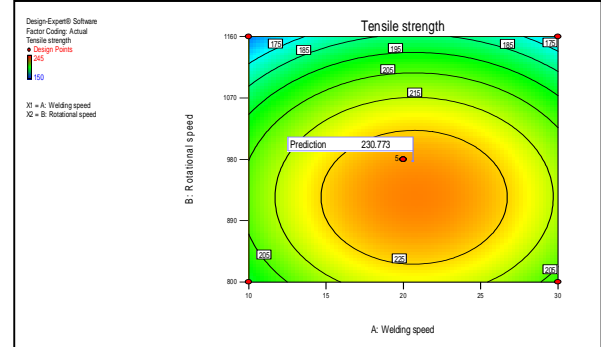
Fig. 20. The optimum value of Tensile strength.
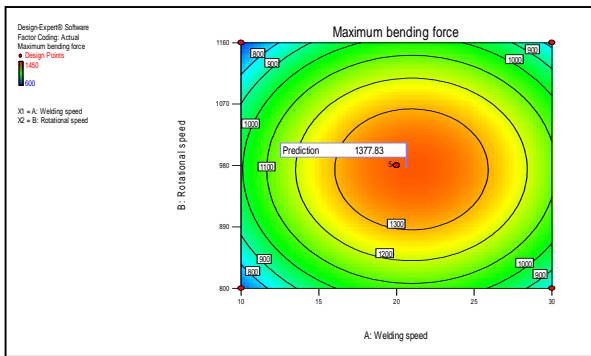
Fig. 21. The optimum value of Maximum bending force.

Notation

A   welding speed
B   rotational speed
C_p specific heat
k   thermal conductivity

Greek Letters

ρ   density
α   star point

7. References

[1] Rajif S. Mishra and Murray W. Mahoney, "Friction Stir Welding and Processing", Wiley Inc., 2007.

[2] R. Palanivel, P. Mathews, N. Muragan, and I. Dinaharan, "Effect of Tool Rotational Speed and Pin Profile on Microstructure and Tensile Strength of Dissimilar Friction Stir Welded AA5083-H111 and AA6351-T6 Aluminum Alloys", Journal of Materials and Design, Vol. 40, pp. 7-16, 2012.

[3] I. Rani and R. Marpu, "The Effect of Variation of Tool Geometry on Friction Stir Welded Aluminum Alloys- An Experimental Investigation", International Journal of Mechanical Engineering and Robotics Research, Vol. 1, No. 1, pp. 91-98, 2012.

[4] H. Mohanty, D. Venkateswarlu, M. Mahapatra, P. Kumar and N. Mandal, "Modeling the Effects of Tool Probe Geometries and Process Parameters on Friction Stirred Aluminum Welds", Journal of Mechanical Engineering and Automation, Vol. 2(4), pp. 74-79, 2012.

[5] R. Narsu and I. Rani, "An Experimental Investigation of the Effect of Variation of Tool Geometry And Optimization of Process Parameters on Friction Stir Welded Aluminum Alloys", International Journal of Research in Aeronautical and Mechanical Engineering, Vol. 1, Issue. 7, pp. 261-266, 2013.

[6] M. Koilraj, V. Sundareswaran, S. Vijayan, and S. Rao, "Friction stir Welding of Dissimilar Aluminum Alloys AA2219 to AA5083- Optimization of Process Parameters Using Taguchi Technique", Journal of Materials and Design, Vol. 42, pp. 1-7, 2012.

[7] P. Prasanna, C. Penchalayya, and D. Rao, "Optimization and Validation of Process Parameters in Friction Stir Welding on AA6061 Aluminum Alloy Using Gray Relational Analysis", International Journal of Engineering Research and Applications (IJERA), Vol. 3, Issue. 1, pp. 1471-1481, 2013.

[8] Standard Specification for Aluminum and Aluminum Alloy ASTM Sheet and Plate, ASTM B209M.

[9] Standard JIS G 4404, Alloy Tool Steel, Material Number 1.208, 1983.

[10] Standard Test Method for Tension Testing of Metallic Materials, ASTM E8M, 1988.

[11] Standard Method for Guided Bend Test for Ductility of Welds, ASTM E190, 1980.

[12] Montgomery, D. C., "Design and Analysis of Experiments", 5th Edition, John Wiley & Sons Inc., 2000.

[13] A. Aggarwal and H. Singh, "Optimization of Machining Techniques - A Retrospective and Literature Review", Sadhana, Vol. 30, Part 6, pp. 699-711, 2005.

[14] Huijie Liu, Huijie Zhang, Qing Pan, and Lei Yu, "Effect of FSW Parameters on Microstructural Characteristics and Mechanical Properties of 2219-T6 Aluminum Alloy Joints", International Journal of Material Forming, Vol. 5, pp. 235-241, 2012

تحديد معاملات اللحام المثالية لسبائك الالمنيوم (AA2024-T351) الملحومة بواسطة لحام الخلط الاحتكاكي

سمير علي أمين الربيعي*   قاسم عباس عطية**   زهير الطاهر***

*،**،***قسم الهندسة الميكانيكية / الجامعة التكنولوجية

*البريد الالكتروني: alrabiee2002@yahoo.com

**البريد الالكتروني: dr_qasim_uot@yahoo.com

***البريد الالكتروني: zuhairsadeed@gmail.com

الخلاصة

اللحام بالخلط الاحتكاكي هو عملية لحام جديدة نسبياً، و الذي يستلزم لحام المعادن بدون استخدام الانصهار او المواد المالئة. في هذه الدراسة، تم التحقق من تاثير معاملات اللحام على الخواص الميكانيكية لسبائك الالمنيوم (AA2024-T351) الملحومة بطريقة لحام الخلط الاحتكاكي.

تم استخدام مديات مختلفة لمعاملات اللحام، بوصفها عوامل إدخال، مثل سرعة اللحام (6-34 mm/min) و السرعة الدورانية (725-1235 rpm) للحصول على تاثيرها على الاستجابات الرئيسة، بدلالة الاستطالة و مقاومة الشد، و قوة الانحناء العظمى. كما قد تم إستخدام و تحليل قياسات تجريبية للاستطالة، مقاومة الشد، وقوة الانحناء العظمى بإستعمال برنامج التصميم التجريبي (DESIGN EXPERT 8) للحصول على نماذج منهجية للاستجابة السطحية (RSM). كما تم إستحصال و تحليل النموذج الرياضي للإستجابات (الاستطالة، مقاومةالشد، وقوةالانحناءالعظمى) كدوال لضروف اللحام المستعملة باستعمال تباين ANOVA للتحقق من ملائمة هذه النماذج. النماذج المربعة الناتجة بينت بانه بزيادة سرعة اللحام و السرعة الدورانية، فانه تزداد مقاومة الشد و الاستطالة الى قيمة عظمى في البداية ثم تتناقص بسبب حدوث العيوب الفراغية. كما ان زيادة كلا من سرعة اللحام والسرعة الدورانية تؤدي الى زيادة قوة الانحناء العظمى اولاً الى قيمة عظمى ثم تتناقص. ومهما يكن من امر، فقد وجد بان سرعة اللحام تكون اكثر تاثيرا من السرعة الدورانية. و وجد توافق جيد بين نتائج هذه النماذج و الامثلية مع النتائج العملية بمستوى ثقة (95%).